Clays and Clay Minerals, Vol. 57, No. 2, 271–277, 2009.

MELT SYNTHESIS AND CHARACTERIZATION OF SYNTHETIC Mn-RICH TAINIOLITE

ALEXANDER BAUMGARTNER, CHRISTIAN BUTTERHOF, SEBASTIAN KOCH, RUSLAN MARIYCHUK, AND JOSEF BREU*

Department of Inorganic Chemistry I, University of Bayreuth, 95447 Bayreuth, Germany

Abstract—Large transition-metal contents add desirable physical properties, such as redox reactivity, magnetism, and electric or ionic conductivity to micas and make them interesting for a variety of materials-science applications. A Mn- and F-rich tainiolite mica, $Cs(Mn_2^{2+}Li)Si_4O_{10}F_2$, was synthesized by a high-temperature melt-synthesis technique. Subsequent annealing for 10 days led to a single-phase and coarse-grained material. Single-crystal X-ray diffraction studies were performed and characteristic geometric parameters were compared to the analogous ferrous compound, synthetic Fe-rich tainiolite, $Cs(Fe_2^{2+}Li)Si_4O_{10}F_2$. Both tainiolite structures are outside the compositional stability limits for the 2:1 layer structure, and incorporating the relatively large cation Mn^{2+} requires significant structural adjustments in both the octahedral and tetrahedral sheets. As expected, increasing the ionic radius of the octahedral cation from 0.78 Å ($^{VI}Fe^{2+}$) to 0.83 Å ($^{VI}Mn^{2+}$) reduces the octahedral flattening angle from $<\Psi> = 57.05°$ to $<\Psi> = 56.4°$, the smallest value ever observed for a tetrasilicic mica. However, even this small $<\Psi>$ value is insufficient to match the lateral sizes of the tetrahedral and octahedral sheets and, in addition, unusual structural adjustments in the tetrahedral sheet are required. The average tetrahedral bond length $<T–O>$ is much greater (1.643 Å) than the average value observed for tetrasilicic micas (1.607 Å,) and a significant difference between the $<T–O>_{apical}$ (1.605 Å) and the $<T–O>_{basal}$ bond lengths (1.656 Å) and an enlarged basal flattening angle ($\tau_{bas} = 106.29°$) are noted. These parameters indicate: (1) that the 2:1 layer might be more flexible than previously thought, to allow matching of the lateral dimensions of the tetrahedral and octahedral sheets; and (2) that many other compositions that appear interesting from a materials-science point of view might be accessible.

Key Words—Crystal Chemistry, Manganese, Mica, Synthetic Clays, Tainiolite.

INTRODUCTION

Micas are widespread in a variety of rocks. Their crystal structure is capable of incorporating an abundance of elements. Several recent surveys and reviews have been published (Brigatti and Guggenheim, 2002; Fleet, 2003; Tischendorf *et al.*, 2007). Upper substitutional limits, in particular for transition metals, have been studied in detail for synthetic and natural micas. The linkage between octahedral and tetrahedral sheets in the mica structure occurs by distortions *via* tetrahedral rotation and octahedral flattening (Hazen and Wones, 1978; Mercier *et al.*, 2006).

Phyllosilicates containing transition metals are interesting because of potential material-science aspects; those with 2:1 layers, represent a stable but flexible inorganic structure, whereas large amounts of transition metals add desirable physical properties, such as magnetism and electric or ionic conductivity (Mariychuk *et al.*, 2007; Rancourt *et al.*, 2001; Ruscher and Gall, 1995, 1997). Moreover, the synthetic Fe-rich tainiolite, $Cs(Fe_2^{2+}Li)Si_4O_{10}F_2$, can be converted into a porous hybrid material by oxidative pillaring (Baumgartner *et al.*, 2008; Tsapatsis and Maheshwari, 2008).

Despite these attractive properties, only a small number of synthetic phyllosilicates with large transition-metal contents are known (Comodi *et al.*, 1999; Hazen and Wones, 1972; Ihara and Kitajima, 1997; Kitajima *et al.*, 1995; Redhammer *et al.*, 2005; Tischendorf *et al.*, 2007) and these contain mainly Co^{2+}, Ni^{2+}, $Fe^{2+/3+}$, and Zn^{2+} as transition metals. Natural micas usually contain only small amounts of Mn^{2+}.

Synthesis of trioctahedral micas with Mn-bearing starting materials suggests that micas with a tetrahedral composition of (Si_3Al) cannot contain more than ~1 $^{VI}Mn^{2+}$ per formula unit (Hazen and Wones, 1972). Micas containing dominant, octahedrally coordinated Mn^{2+} have been reported for shirozulite (Ishida *et al.*, 2004). However, the chemical composition of the crystal investigated was quite different from the ideal, end-member composition $KMn_3^{2+}(AlSi_3)O_{10}(OH)_2$. The composition observed has a mean constituent octahedral cation radius that falls below the critical limit of 0.76 Å as suggested by Hazen and Wones (1972).

The smaller tetrahedral sheet in tetrasilicic compositions decreases the critical radius to 0.73 Å (Eggleton and Ashley, 1989; Guggenheim and Eggleton, 1987). Whereas norrishite, $K(Mn_2^{3+}Li)Si_4O_{10}(O)_2$ (Eggleton and Ashley, 1989; Gnos *et al.*, 2003; Tyrna and Guggenheim, 1991), is found in nature, the analogous synthetic Mn^{2+}-

* E-mail address of corresponding author:
josef.breu@bayreuth.de
DOI: 10.1346/CCMN.2009.0570213

rich mica is expected to be unstable based on the misfit between the tetrahedral and octahedral sheets. These geometrical constraints are expected to inhibit the incorporation of the much larger Mn^{2+} cations (Hazen and Wones, 1978). Synthesis of Mn^{2+}-rich phyllosilicates is, therefore, believed to be impossible.

Higashi *et al.* (2007) were, however, able to synthesize smectites with larger amounts of Mn^{2+}: $(Na_{0.4}(Mn_{2.6}Li_{0.4})Si_4O_{10}(OH)_2$, $Na_{0.4}Mn_{2.8}Si_4O_{10}(OH)_2$, and $Na_{0.4}Mn_3(Si_{3.6}Al_{0.4})Si_4O_{10}(OH)_2$).

The current study presents the preparation of a phase-pure Mn^{2+}-rich synthetic fluoromica, Mn-rich tainiolite, $Cs(Mn_2^{2+}Li)Si_4O_{10}F_2$, which was synthesized *via* a high-temperature technique. The structural adjustments required by the incorporation of large amounts of the Mn^{2+} cation are discussed.

MATERIALS AND METHODS

High-purity reagents (in total ~50 g) of CsF (Aldrich, 99.9%), LiF (Aldrich, 99.9%), SiO_2 (Merck, fine granular, calcined), and MnO were weighed in an Ar atmosphere in accordance with a stoichiometric composition for $Cs(Mn_2^{2+}Li)Si_4O_{10}F_2$. To obtain a stoichiometric composition of MnO, commercially available MnO (Aldrich, 99%) was annealed at 1130ºC in a $CO:CO_2$ = 1:1 gas atmosphere prior to weighing. The molybdenum crucible was sealed so as to be gas tight using the procedure of Breu *et al.* (2001). The Mo crucible also acted as an oxygen buffer.

The crucible was heated in a graphite furnace (Graphit HT-1900, Linn High Therm) for the synthesis. To prevent inhomogeneity of material owing to gravity segregation in the melt, the crucible was positioned horizontally in the furnace and rotated at 60 rpm. The crucible was heated from room temperature (RT) to 1750ºC (15ºC min^{-1}), left at 1750ºC for 2 h, cooled to 800ºC (50ºC min^{-1}), and then quenched by switching off the power. To improve the crystallinity and increase the crystal sizes in the bulk material, the product was ground and further annealed in a smaller, gas-tight, sealed Mo crucible according to the following temperature sequence: heating from RT to 700ºC (10ºC min^{-1}), heating to 770ºC (1ºC min^{-1}), annealing at 770ºC for 10 days, cooling to 400ºC (0.3ºC min^{-1}), and quenching by switching off the power.

Powder X-ray diffraction (PXRD) patterns (*e.g.* Figure 1) were recorded using a STOE Stadi P powder diffractometer (transmission geometry, CuKα radiation (λ = 1.54056 Å), Ge monochromator, linear, position-sensitive scintillation detector). The measurement was done using a glass capillary to minimize texture. A Le Bail fit as implemented in *TOPAS* (Coelho, 2003) was employed to refine the unit cell and to extract the observed intensities. Because of the massive peak overlap, the fit was limited to 50º2θ. Intensities extracted from the PXRD pattern were compared to intensities calculated on the basis of the single-crystal structure refinement (Table 1). Single-crystal X-ray data were collected on a crystal free from diffuse streaks related to stacking disorder. Data were collected at 298 K on a STOE IPDS diffractometer with graphite-monochromated MoKα radiation (λ = 0.71073 Å) using a crystal 0.28 mm × 0.35 mm × 0.04 mm in size in 90 frames (2º step per frame, 20 min per frame). Further details of the data collection and structure refinement are given in Table 2.

The chemical composition of the synthetic Mn-rich tainiolite was determined by wavelength dispersive X-ray spectroscopy (WDX) using an electron microprobe (Jeol JXA-8200, at Bayerisches Geoinstitut, Bayreuth, Germany) operated at the following settings: acceleration voltage 15 kV, initial probe current 15 nA, and a beam spot diameter of 1 µm. Measured intensities were normalized by reference to standard materials (pollucite for Cs, $MnTiO_3$ for Mn, andradite for Si, MgO for O, and fluorite for F). The counting time was 20 s at the peak position and 10 s on each side of the peak position. Because of the inability of this method to determine the Li content, the composition was normalized to $Si_{4.00}$ and then further normalized to 22 negative charges according the composition $Si_{4.00}O_{10}F_2$. The estimated standard deviation values for the composition were calculated using this normalization method as determined from the error values obtained from the measurements.

The Li content was verified by laser ablation-inductively coupled plasma-mass spectrometry (LA-ICP-MS). The LA-ICP-MS system consisted of an Elan DRC-e quadrupole mass spectrometer (PerkinElmer Instruments) attached to a Geolas M 193 nm ArF Excimer Laser system (Coherent/ Lambda Physik) (see Gunther *et al.*, 1997). Samples were pressed to pellets without additives. Ablation involved laser-beam sizes from 5 to 20 µm in diameter. The laser was operated at a frequency of 10 Hz at 25 kV. The sample

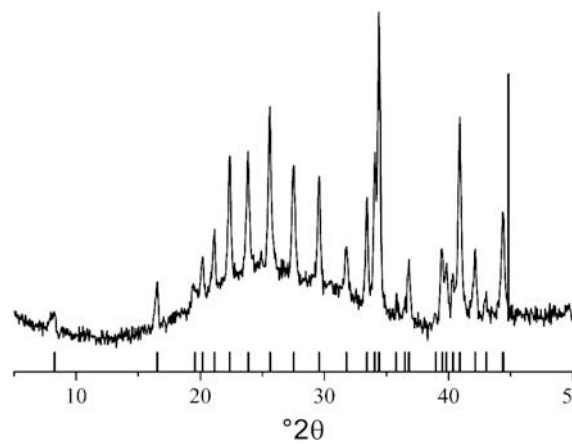

Figure 1. Powder X-ray diffraction pattern of Mn-rich synthetic tainiolite $CsMn_2^{2+}LiSi_4O_{10}F_2$.

https://doi.org/10.1346/CCMN.2009.0570213 Published online by Cambridge University Press

Table 1. Peak list for the PXRD of synthetic Mn-rich tainiolite.

Position (°2θ)	*d* value (Å)	*h*	*k*	*l*	Relative intensity (%, calc)	Relative intensity (%, *TOPAS*)
8.25	10.71	0	0	1	8.8	6.1
16.54	5.36	0	0	2	14.8	22.4
19.60	4.52	1	1	0	6.0	2.7
20.18	4.40	1	1	−1	20.0	18.0
21.14	4.20	0	2	1	30.8	26.4
22.37	3.97	1	1	1	68.2	62.0
23.87	3.73	1	1	−2	79.9	58.7
25.62	3.47	0	2	−2	100.0	76.4
27.52	3.24	1	1	2	77.6	68.3
29.58	3.02	1	1	−3	62.1	61.1
31.79	2.81	0	2	−3	30.6	28.4
33.44	2.68	0	0	4	27.4	61.2
34.05	2.63	2	0	−1	12.3	24.5
34.09	2.63	1	1	3	45.5	25.7
34.41	2.60	2	0	0	33.6	100.0
34.44	2.60	1	3	−1	67.1	66.5
35.77	2.51	1	3	1	5.8	1.1
36.47	2.46	1	1	−4	5.9	1.6
36.79	2.44	2	0	1	6.6	17.6
36.81	2.44	1	3	−2	12.8	14.9
38.96	2.31	0	2	4	4.1	0.0
39.50	2.28	2	2	−1	15.8	24.6
39.81	2.26	2	2	0	18.1	31.3
40.36	2.23	0	4	1	13.3	24.1
40.89	2.21	2	0	2	23.5	65.2
40.90	2.20	1	3	−3	46.7	48.6
42.15	2.14	0	0	5	12.8	33.6
43.04	2.10	0	4	−2	8.5	0.2
44.41	2.04	1	3	3	30.1	31.3
44.37	2.04	2	0	−4	14.9	28.9

Unit cell refined in *C*2/*m* (No.12): a = 5.279(1) Å; b = 9.132(0) Å; c = 10.854(2) Å; β = 99.35(1)°; V = 516.32 Å^3

chamber was flushed with He gas and Ar gas was added to the vapor stream. Signals were recorded with five sweeps per second, and instrument background was measured for 30 s before each analysis. Integrated signal intensities were referenced to NIST SRM 610 glass according to routines described elsewhere (Longerich *et al.*, 1996). Element ratios were converted to stoichiometric coefficients by normalization to $Si_{4.00}$.

Differential scanning calorimetry (Figure 2) to determine the melting point of the Mn-rich synthetic tainiolite was performed using a Netzsch STA 449 C Jupiter DSC instrument (50−1000°C, 10°C min^{-1}, Ar atmosphere, ~100 mg sample weight in a custom-made, gas-tight, sealed Pt/Ir 97/3 crucible on a sapphire disc).

RESULTS

Synthesis

The synthesized compound was greenish in color and contained crystals with plate-like shape and up to 1 mm in diameter.

The chemical composition was $Cs_{0.99(1)}(Mn_{2.05(5)}Li_{0.91(15)})Si_4O_{10}F_2$ and $Cs_{0.95(5)}(Mn_{1.94(10)}Li_{1.03(5)})Si_4O_{10}F_2$, as determined by WDX and LA-ICP-MS, respectively.

According to the PXRD pattern (Figure 1, Table 1), no impurity was detectable and all peaks could be refined with the unit cell of Mn-rich synthetic tainiolite given in Table 1. Note that the broad background intensity in the range 20−30°2θ indicates an X-ray amorphous phase which can be attributed to the glass

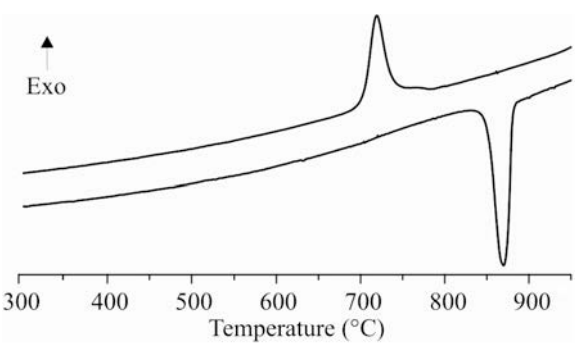

Figure 2. Differential scanning calorimetry curve of Mn-rich synthetic tainiolite $Cs(Mn_2^{2+}Li)Si_4O_{10}F_2$.

https://doi.org/10.1346/CCMN.2009.0570213 Published online by Cambridge University Press

capillary. The quality of the Le Bail profile fit was good (wRp = 3.73 %). Nevertheless, the relative intensities extracted from the PXRD pattern were significantly affected by texture and peak overlap (Table 1).

In contrast to hydrothermal techniques, where control of the valence state of Mn is difficult, the oxygen fugacity required for Mn^{2+} is fixed during the melt-synthesis method because the crucible material Mo/MoO_x acts as an oxygen fugacity buffer.

Mn^{2+}-containing silicate melts tend to produce glass and thus the complete crystallization of the melt into the desired mica phase is difficult. The lengthy annealing process near the melting point of Mn-rich synthetic tainiolite was crucial and finally produced complete crystallization of the bulk material. No glass transition signal in the DSC plot was detected. The melting point, as determined by the DSC measurement, was 791ºC (Figure 2).

The experimental details and results of the single-crystal structure refinement are summarized in Tables 2 and 3. Selected geometric parameters of the synthetic Mn-rich tainiolite are listed in Table 4. Further information about the structure refinement may be requested from Fachinformationszentrum Karlsruhe, Gesellschaft für wissenschaftlich-technische Information mbH, D-76344 Eggenstein-Leopoldshafen, Germany, by indicating the deposition number CCDC-419899 (E-mail: crysdata@fiz-karlsruhe.de).

Table 2. Crystallographic data and details of the structure determination of synthetic, Mn-rich tainiolite.

Crystal data
- M_r = 560.09
- MoKα radiation (λ = 0.71073 Å)
- T = 298 K
- a = 5.3013(11) Å
- b = 9.1761(18) Å
- c = 10.878(2) Å
- β = 99.15(3)º
- V = 522.44(18) Å^3
- Monoclinic. *C2/m* (No. 12)
- Cell parameters from
- Z = 2
- μ = 6.39 mm^{-1}
- Plate greenish
- 0.28 mm × 0.35 mm × 0.04 mm
- D_x = 3.560 Mg m^{-3}

Data collection
- STOE IPDS I diffractometer
- Radiation source: fine-focus sealed tube
- Monochromator: graphite
- T = 293(2) K
- Absorption correction: numerical, *via* equivalents
- 1315 measured reflections
- 757 independent reflections
- 685 reflections with $I > 2\sigma(I)$
- R_{int} = 0.042
- θ_{max} = 29.9º
- θ_{min} = 3.8º
- h = −7→7
- k = −12→11
- l = 0→15

Refinement
- Refinement on F^2
- $R[F^2 > 2\sigma(F^2)]$ = 0.048
- $wR(F^2)$ = 0.157
- S = 1.39
- 757 reflections
- $w = 1/[\sigma^2(F_o^2) + (0.0511P)^2 + 13.4087P]$ where $P = (F_o^2 + 2F_c^2)/3$
- $\Delta\rho_{max}$ = 2.11 e Å^{-3}
- $\Delta\rho_{min}$ = −0.91 e Å^{-3}
- $(\Delta/\sigma)_{max} < 0.001$
- 57 parameters

DISCUSSION

The fit of the lateral dimensions of the tetrahedral and octahedral sheets is a convincing argument for the stability of 2:1 phyllosilicate structures. The dimensions are mainly determined by the ionic radii of the structural cations and, therefore, by the chemical composition of the sheets. Slight misfits in the dimensions can be compensated by structural-adjustment mechanisms (Brigatti and Guggenheim, 2002). Despite their significance for the stability of phyllosilicates, predicting the actual structural adjustments is difficult. As a first approximation, the following stability considerations concerning the synthetic Mn-rich tainiolite structure ignore these adjustment mechanisms and are based solely on the pronounced dependence of the sheet dimensions on the chemical composition.

For the synthetic Mn-rich tainiolite, sheet-size calculations based on the equations of Donnay *et al.* (1964) and Hazen and Wones (1978) show that the lateral dimension of the octahedral sheet is too large to fit the dimension of the tetrahedral sheet. Assuming a non-corrugated tetrahedral sheet and ideal tetrahedral symmetry, the tetrahedral rotation angle, α, can be correlated to the cation−anion distance in the octahedral sheet, d_o, the octahedral flattening angle, Ψ, and the cation−anion distance in the tetrahedral sheet, d_t, in the following way:

$$\cos\alpha = \sqrt{3}d_o \sin\Psi / 4\sqrt{2}d_t \quad (1)$$

$$\sin\Psi \approx 1.154 - 0.144 d_o \quad (2)$$

The maximum lateral expansion of the mica structure is achieved when the tetrahedral sheet is fully expanded (α = 0º). For the given composition of synthetic Mn-rich tainiolite, $\langle d_t \rangle$ = 1.61 Å and $\langle d_o \rangle$ = 2.121 Å may be derived using Shannon radii. Fixing α = 0º and substituting these values into equation 1, $\langle \Psi_{exp.} \rangle$ would be expected to be 55.1º. Usually, the values for the octahedral flattening angles $\langle \Psi \rangle$ for micas are 59−60º (Weiss *et al.*, 1985). The octahedral flattening angle observed for synthetic Mn-rich tainiolite is much

https://doi.org/10.1346/CCMN.2009.0570213 Published online by Cambridge University Press

Table 3. Atomic coordinates and displacement factors of synthetic Mn-rich tainiolite.

Atom	Site	Occupancy	x	y	z	$U_{eq} \times 10^2$	$U_{11} \times 10^2$	$U_{22} \times 102$	$U_{33} \times 10^2$	$U_{12} \times 10^2$	$U_{13} \times 102$	$U_{23} \times 10^2$
Cs	2a	1	0	0	0	2.42(4)	2.33(5)	2.228(6)	2.68(6)	0	0.52(4)	0
*M*1	2d	0.723(16) Mn^{2+}	½	0	½	1.70(11)	1.89(16)	1.60(19)	1.69(16)	0	0.57(11)	0
		0.280(20) Li^{+}										
*M*2	4h	0.587(12) Mn^{2+}	0	0.1660(3)	½	1.79(10)	1.73(14)	1.74(17)	1.87(14)	0	0.21(9)	0
		0.413(17) Li^{+}										
Si	8j	1	0.0804(4)	0.2397(2)	0.2397(2)	1.44(5)	1.29(8)	1.34(11)	1.71(9)	−0.01(7)	0.34(7)	0.02(7)
O1	8j	1	0.1300(11)	0.3332(7)	0.3891(5)	1.88(11)	2.1(3)	1.9(3)	1.6(2)	0.0(2)	0.5(2)	−0.1(2)
O2	4i	1	−0.4402(15)	0	0.1812(8)	1.88(15)	2.3(4)	1.1(4)	2.3(4)	0	0.4(3)	0
O3	8j	1	0.1897(9)	0.2496(7)	−0.1805(5)	1.76(11)	1.4(2)	2.0(3)	1.9(3)	0.3(2)	0.3(2)	0.0(2)
F	4i	1	0.1288(14)	0	0.3927(7)	2.59(15)	2.6(3)	2.3(4)	3.0(4)	0	0.6(3)	0

smaller (<$\Psi_{obs.}$> = 55.8°, Table 5), which results in an increase in the thickness of the octahedral sheet. The octahedral flattening angle is considerably less than the supposed limiting value of <Ψ> = 58.2° suggested by Redhammer *et al.* (2005). Nevertheless, even this small <Ψ> value is still slightly larger than the value expected for topological reasons (equation 1, <$\Psi_{exp.}$> = 55.1°), probably because shared O−O edges of a polyhedron are generally shorter than unshared edges, and the *M*−F bond length is generally shorter than the *M*−O bond length (Table 4). Thus, a further decrease in the octahedral flattening angle is limited. Reducing the octahedral flattening angle below the limit proposed by Redhammer *et al.* (2005), nonetheless, is essential. However, minimizing the tetrahedral rotation and the octahedral flattening is not yet sufficient to match the lateral sizes of the tetrahedral and octahedral sheets. Consequently, for synthetic Mn^{2+}-rich tainiolite, additional adjustment mechanisms must occur, which will be discussed below.

Characteristic structural parameters, as derived from the atomic coordinates obtained from the single-crystal XRD refinements, for synthetic Mn-rich tainiolite were compared (Table 5) with the parameters of synthetic Fe-rich tainiolite (Mariychuk *et al.*, 2007) and natural norrishite (Tyrna and Guggenheim, 1991). The parameters observed for synthetic Mn-rich tainiolite follow the trend expected for increasing ionic radii of the octahedral cations. Going from 0.65 Å ($^{VI}Mn^{3+}$) to 0.78 Å ($^{VI}Fe^{2+}$) and to 0.83 Å ($^{VI}Mn^{2+}$) (all Shannon radii, high-spin state (Shannon, 1976)), the value of the octahedral flattening angle, <Ψ>, decreases to gradually shrink the lateral extension of the octahedral sheet and concomitantly increase its thickness. For both synthetic phases, the tetrahedral sheet is of course near to its maximum lateral extension (α = 0°). This lower limit for the tetrahedral rotation is probably also affected by the

Table 4. Selected bond lengths of synthetic Mn-rich tainiolite.

Octahedral site	Bond length (Å)
*M*1−O 4×	2.131(6)
*M*1−F 2×	2.118(7)
*M*2−O 4×	2.133(6)
*M*2−F 2×	2.091(6)
Tetrahedral site	
Si−O1	1.604(6)
Si−O2	1.653(4)
Si−O3	1.652(6)
Si−O3	1.662(6)
Interlayer space	
Cs−O2	3.285(8)
Cs−O2	3.291(8)
Cs−O3	3.278(6)
Cs−O3	3.288(6)
Cs−F	4.228(8)

https://doi.org/10.1346/CCMN.2009.0570213 Published online by Cambridge University Press

Table 5. Structural parameters as obtained from the single-crystal structure refinements for synthetic Mn-rich tainiolite (this work). Synthetic Fe-rich tainiolite (Mariychuk *et al.*, 2007) and norrishite (Tyrna and Guggenheim, 1991).

Parameter		Mn-rich tainiolite	Fe-rich tainiolite	Norrishite
Unit cell *C2/m* (No. 12)	*a*	5.301(1) Å	5.277(2) Å	5.289(3) Å
	b	9.176(2) Å	9.158(2) Å	8.914(3) Å
	c	10.878(2) Å	10.804(2) Å	10.062(7) Å
	β	99.15(3)º	99.19(3)º	98.22(5)º
<*M*1−O.F>. $d_{o.M1}$		2.126 Å	2.098 Å	2.123 Å
<*M*2−O.F>. $d_{o.M2}$		2.119 Å	2.098 Å	2.040 Å
<*M*−O.F>. <d_o>		2.121 Å	2.098 Å	2.068 Å
Octahedral sheet height h_o		2.349 Å	2.282 Å	2.215 Å
Octahedral flattening angle *M*1 Ψ_{M1}		56.47º	57.05º	58.56º
Octahedral flattening angle *M*2 Ψ_{M2}		56.34º	57.05º	57.12º
Mean octahedral flattening angle <Ψ>		56.38º	57.05º	57.62º
<*T*−O>$_{apical}$		1.605 Å	1.597 Å	1.571 Å
<*T*−O>$_{basal}$		1.656 Å	1.649 Å	1.636 Å
<*T*−O>.<d_t>		1.643 Å	1.636 Å	1.620 Å
Tetrahedral rotation angle α		0.26º	0.14º	0.6º
Mean basal flattening angle <τ_{bas}>		106.29º	106.34º	105.9º

Definition of parameters as determined using the results of the single-crystal structure refinements:
<*M*1−O.F>: mean cation−anion distance in the octahedral *trans* site
<*M*2−O.F>: mean cation−anion distance in the octahedral *cis* site
<*M*−O.F>: mean cation−anion distance in the octahedral sheet (<*M*1−O.F> + 2·<*M*2−O.F>)/3
<*T*−O>: mean cation−anion distance in the tetrahedral sheet
<τ_{bas}>: mean angle O_{basal}−Si−O_{basal}
h_o: 2 *c* sin(β) [½ − (Fz + 2·O1z)/3]
$\Psi_{M1;M2}$: arccos[$h_0/2d_{o.M1;M2}$]
<Ψ>: (Ψ_{M1} + Ψ_{M2})/3
α: ⅙ $\Sigma_{i=1}^{6}|120^o - \phi_i|$ with ϕ_i being the angle between the the bridging basal tetrahedral oxygen cations

large interlayer cation (Cs^+). The large interlayer cation partly resides in the hexagonal cavities of the tetrahedral sheets and helps to enlarge the cavity to its maximum size, thereby further stretching the tetrahedral sheet. As a consequence of this maximum lateral extension state of the tetrahedral sheet, the interlayer cation Cs^+ exhibits a 6+6 coordination, in close agreement with the observed tetrahedral rotation angle and the coordination numbers usually observed for tainiolites (Weiss *et al.*, 1992). The Cs−O bond lengths, as determined from the single-crystal structure refinement, have almost equal values, indicating that the interlayer cation site is close to ideal hexagonal symmetry.

Surprisingly, the average tetrahedral bond length <*T*−O> is much greater (1.643 Å) than the average value observed for natural samples (1.607 Å) (Brigatti and Guggenheim, 2002). In addition to minimizing tetrahedral rotation and octahedral flattening, structural adjustments within the tetrahedral sheet represent a third mechanism to help match the lateral sizes of the tetrahedral and octahedral sheets. Such adjustments are most obvious in terms of the significant difference between the <*T*−O>$_{apical}$ and the <*T*−O>$_{basal}$ bond lengths (Table 5). As a consequence, the lateral extension of the tetrahedral sheet is enlarged and the tetrahedral basal flattening angle <τ_{bas}> is increased, also reflected in the considerably larger *a* and *b* axes of both synthetic Mn-rich and synthetic Fe-rich tainiolite as compared to equivalent values for norrishite.

ACKNOWLEDGMENTS

This work was supported financially by the graduate school 'Structure, Reactivity and Properties of Oxide Materials' within the Elitenetzwerk Bayern and the Deutsche Forschungsgemeinschaft (DFG, BR1408/5). The authors thank the Bayerisches Geoinstitute, Bayreuth, Germany, for the WDX and LA-ICP-MS measurements. The authors are also grateful to reviewer Dr S. Guggenheim.

REFERENCES

Baumgartner, A., Sattler, K., Thun, J., and Breu, J. (2008) A route to microporous materials through oxidative pillaring of micas. *Angewandte Chemie-International Edition*, **47**, 1640−1644.

Breu, J., Seidl, W., Stoll, A.J., Lange, K.G., and Probst, T.U. (2001) Charge homogeneity in synthetic fluorohectorite. *Chemistry of Materials*, **13**, 4213−4220.

Brigatti, M.F. and Guggenheim, S. (2002) Mica crystal chemistry and the influence of pressure, temperature, and solid solution on atomistic models. 1−97 in: *Micas: Crystal Chemistry & Metamorphic Petrology* (A. Mottana, F.P. Sassi, J.B. Thompson Jr., and S. Guggenheim, editors).

Reviews in Mineralogy & Geochemistry, **46**. Mineralogical Society of America and the Geochemical Society, Washington, DC.

Coelho, A.A. (2003) *TOPAS User's Manual*, Version 3.1, Bruker AXS, GmbH, Karlsruhe, Germany.

Comodi, P., Zanazzi, P.F., Weiss, Z., Rieder, M., and Drabek, M. (1999) "Cs-tetra-ferri-annite": High-pressure and high-temperature behavior of a potential nuclear waste disposal phase. *American Mineralogist*, **84**, 325–332.

Donnay, G., Takeda, H., and Donnay, J.D.H. (1964) Trioctahedral 1-layer micas. II. Prediction of structure from composition and cell dimensions. *Acta Crystallographica*, **17**, 1374–1381.

Eggleton, R.A. and Ashley, P.M. (1989) Norrishite, a new manganese mica, $K(Mn_2^{3+}Li)Si_4O_{12}$, from the Hoskins Mine, New South Wales, Australia. *American Mineralogist*, **74**, 1360–1367.

Fleet, M.E. (2003) *Rock-Forming Minerals Vol. 3A – Micas*. The Geological Society, London.

Gnos, E., Armbruster, T., and Villa, I.M. (2003) Norrishite, $K(Mn_2^{3+}Li)Si_4O_{10}(O)_2$, an oxymica associated with sugilite from the Wessels Mine, South Africa: Crystal chemistry and Ar-40-Ar-39 dating. *American Mineralogist*, **88**, 189–194.

Guggenheim, S. and Eggleton, R.A. (1987) Modulated 2-1 layer silicates – review, systematics, and predictions. *American Mineralogist*, **72**, 724–738.

Gunther, D., Frischknecht, R., Heinrich, C.A., and Kahlert, H.J. (1997) Capabilities of an argon fluoride 193 nm excimer laser for laser ablation inductively coupled plasma mass spectrometry microanalysis of geological materials. *Journal of Analytical Atomic Spectrometry*, **12**, 939–944.

Hazen, R.M. and Wones, D.R. (1972) Effect of cation substitutions on physical properties of trioctahedral micas. *American Mineralogist*, **57**, 103–129.

Hazen, R.M. and Wones, D.R. (1978) Predicted and observed compositional limits of trioctahedral micas. *American Mineralogist*, **63**, 885–892.

Higashi, S., Miki, H., and Komarneni, S. (2007) Mn-smectites: Hydrothermal synthesis and characterization. *Applied Clay Science*, **38**, 104–112.

Ihara, Y. and Kitajima, K. (1997) Synthesis and properties of Co^{2+}-substituted tetrasilicic fluorine micas. *Journal of the Ceramic Society of Japan*, **105**, 881–885.

Ishida, K., Hawthorne, F.C., and Hirowatari, F. (2004) Shirozulite, $KMn_3^{2+}(Si_3Al)O_{10}(OH)_2$, a new manganese-dominant trioctahedral mica: Description and crystal structure. *American Mineralogist*, **89**, 232–238.

Kitajima, K., Ihara, Y., and Takusagawa, N. (1995) Synthesis and properties of Ni^{2+}-substituted tetrasilicic fluorine micas. *Journal of the Ceramic Society of Japan*, **103**, 1057–1062.

Longerich, H.P., Jackson, S.E., and Gunther, D. (1996) Laser ablation inductively coupled plasma mass spectrometric transient signal data acquisition and analyte concentration calculation. *Journal of Analytical Atomic Spectrometry*, **11**, 899–904.

Mariychuk, R., Baumgartner A., Wagner, F.E., Lerf, A., Dubbe, A., and Breu, J. (2007) Synthesis, structure, and electric conductivity of ferrous tainiolite and its oxidative conversion into coarse-grained swellable smectite. *Chemistry of Materials*, **19**, 5377–5387.

Mercier, P.H.J., Rancourt, D.G., Redhammer, G.J., Lalonde, A.E., Robert, J.L., Berman, R.G., and Kodama, H. (2006) Upper limit of the tetrahedral rotation angle and factors affecting octahedral flattening in synthetic and natural 1M polytype C2/m space group micas. *American Mineralogist*, **91**, 831–849.

Rancourt, D.G., Mercier, P.H.J., Cherniak, D.J., Desgreniers, S., Kodama, H., Robert, J.L., and Murad, E. (2001) Mechanisms and crystal chemistry of oxidation in annite: Resolving the hydrogen-loss and vacancy reactions. *Clays and Clay Minerals*, **49**, 455–491.

Redhammer, G.J., Amthauer, G., Lottermoser, W., Bernroider, M., Tippelt, G., and Roth, G. (2005) X-ray powder diffraction and Fe-57-Mössbauer spectroscopy of synthetic trioctahedral micas $\{K\}[Me_3](TSi_3)O_{10}(OH)_2$, Me = Ni^{2+}, Mg^{2+}, Co^{2+}, Fe^{2+}; T = Al^{3+}, Fe^{3+}. *Mineralogy and Petrology*, **85**, 89–115.

Ruscher, C.H. and Gall, S. (1995) On the polaron-mechanism in iron-bearing trioctahedral phyllosilicates – An investigation of the electrical and optical properties. *Physics and Chemistry of Minerals*, **22**, 468–478.

Ruscher, C.H. and Gall, S. (1997) Dielectric properties of iron-bearing trioctahedral phyllosilicates. *Physics and Chemistry of Minerals*, **24**, 365–373.

Shannon, R.D. (1976) Revised effective ionic-radii and systematic studies of interatomic distances in halides and chalcogenides. *Acta Crystallographica Section A – Foundations of Crystallography*, **32**, 751–767.

Tischendorf, G., Forster, H.J., Gottesmann, B., and Rieder, M. (2007) True and brittle micas: composition and solid-solution series. *Mineralogical Magazine*, **71**, 285–320.

Tsapatsis, M. and Maheshwari, S. (2008) Pores by pillaring: Not always a maze. *Angewandte Chemie – international edition*, **47**, 4262–4263.

Tyrna, P.L. and Guggenheim, S. (1991) The crystal structure of norrishite, $KLiMn_2^{3+}Si_4O_{12}$: n oxygen-rich mica. *American Mineralogist*, **76**, 266–271.

Weiss, Z., Rieder, M., and Chmielova, M. (1992) Deformation of coordination polyhedra and their sheets in phyllosilicates. *European Journal of Mineralogy*, **4**, 665–682.

Weiss, Z., Rieder, M., Chmielova, M., and Krajicek, J. (1985) Geometry of the octahedral coordination in micas – A review of refined structures. *American Mineralogist*, **70**, 747–757.

(*Received 17 October 2008; revised 3 April 2009; Ms. 0215; A.E. J.W. Stucki*)